Russian Journal of Earth Sciences

Arctic Water Current in the Bear Island Trough

E. G. Morozov[1,*], D. I. Frey[1], and A. N. Novigatsky[1]

[1] Shirshov Institute of Oceanology RAS, Moscow, Russia
* **Correspondence to:** Eugene Morozov, egmorozov@mail.ru

Abstract: We analyzed Conductivity-temperature-depth (CTD) and moored Acoustic Doppler Current Profiler (ADCP) measurements in the western Barents Sea carried out onboard the Russian R/V Akademik Mstislav Keldysh (cruise 68) in July–August 2017. A hydrographic section in the Bear Island Trough has been made. Comparison of water properties in the trough and in the sea has been performed. We compared the tidal currents measured on the mooring with those from the TPXO9 model and found that they are quite close.

Keywords: Barents Sea, Norwegian Sea, CTD and ADCP measurements, mooring, tidal ellipses, ocean circulation, tide.

Citation: Morozov, E. G., D. I. Frey, and A. N. Novigatsky (2024), Arctic Water Current in the Bear Island Trough, *Russian Journal of Earth Sciences*, 24, ES4001, EDN: BXWCJO, https://doi.org/10.2205/2024es000925

Introduction

Interaction between dense and cold Arctic waters and relatively warmer Atlantic waters is an important property of the entire North Atlantic region and a key mechanism of climate formation in Russia and whole Europe. The Barents Sea is an important region of strong interaction between these waters. Together with the Fram Strait it contributes to the water mass exchange between the Arctic and Atlantic oceans [*Giraudeau et al.*, 2016]. The Barents Sea is located in a relatively shallow basin north of Europe (Figure 1).

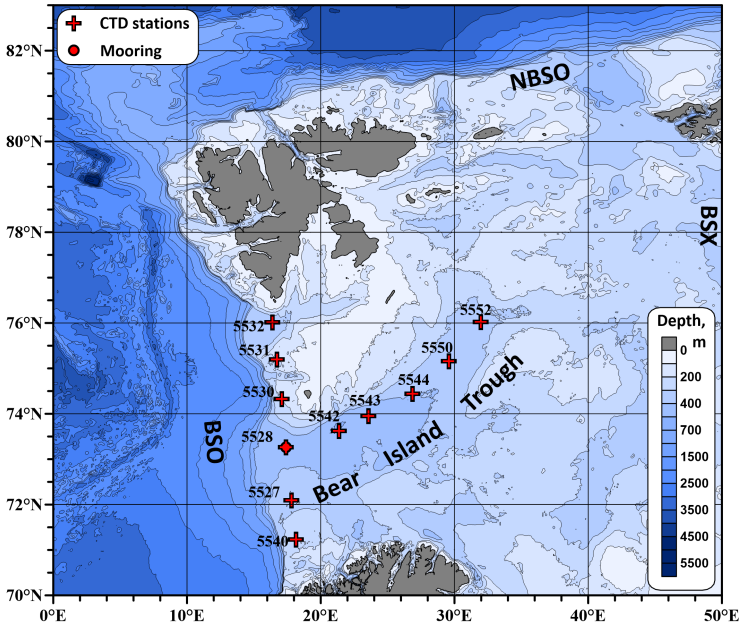

Figure 1. Locations of measurements in the western Barents Sea in July–August 2017. Red crosses show our Conductivity-temperature-depth (CTD) stations; red circle is the site of mooring deployment in the Bear Island Trough. Bathymetry is based on GEBCO 2019 data. Abbreviations: Northern Barents Sea Opening (NBSO); Barents Sea Opening (BSO); Barents Sea Exit (BSX).

Research Article

Received: 2 July 2024
Accepted: 29 July 2024
Published: 9 October 2024

The terms for geographical names in the region are the following: the western boundary of the sea is the Barents Sea Opening (BSO) [*Smedsrud et al.*, 2013]; the northern boundary is the Northern Barents Sea Opening (NBSO) [*Lind and Ingvaldsen*, 2012]. The eastern strait between Franz Josef Land and Novaya Zemlya is the Barents Sea Exit (BSX) [*Gammelsrød et al.*, 2009]. Water exchange occurs through all three boundaries [*Årthun et al.*, 2011].

The Bear Island Trough is the deepest channel for the water exchange between the Norwegian and Barents seas. Its depths reach 500 m; the background depths of the upper parts of its walls are 100–200 meters shallower. The length of the trough exceeds 500 km and its width is approximately 100 km. The slow bottom current of the Deep Barents Sea water in the Bear Island Trough is directed to the Norwegian Sea [*Lukashin and Shcherbinin*, 2007].

The flow of cold and dense Barents Sea waters through the Bear Island Trough is one of the partial sources of Iceland-Scotland Overflow Water (ISOW), which is generally formed in the Norwegian Sea. In winter, cold dense water is formed here due to intense heat transfer to the atmosphere. The water mass that is formed when flowing over the sill in the Faroe-Shetland Channel is called Iceland-Scotland Overflow Water (ISOW). This water mass mixes with the warmer and saltier waters of the Northeast Atlantic. As a result, ISOW turns out to be significantly saltier and warmer than the deep water that penetrates into the Atlantic through the Denmark Strait between Greenland and Iceland (Denmark Strait Overflow Water, DSOW).

In the Atlantic Ocean, North Atlantic Deep Water occupies a layer between 1200 and 4000 m. According to [*Koltermann et al.*, 1999], the densest waters are located in the bottom layers of the Arctic Ocean, but they cannot propagate to the Atlantic owing to the shallow thresholds east of Iceland: Iceland-Faroe and Faroe-Shetland submarine ridges with depths of 480 and 840 m, respectively [*Aken and Boer*, 1995; *Dickson and Brown*, 1994; *Koltermann et al.*, 1999; *Lankhorst and Zenk*, 2006]. A deep (650 m) pathway is also located between Greenland and Iceland.

Waters located above the limiting ridges flow to the Atlantic through the Denmark Strait (Denmark Strait Overflow Water, DSOW) [*Jochumsen et al.*, 2012] and Iceland-Scotland thresholds (Iceland-Scotland Overflow Water, ISOW) [*Mauritzen et al.*, 2005; *Olsen et al.*, 2008]. Iceland-Scotland Overflow Water is formed when water from the Norwegian Sea overflows the thresholds east of Iceland. It is generally accepted that North Atlantic Deep Water is formed as a result of mixing between Labrador Sea Water, Iceland-Scotland Overflow Water, Denmark Strait Overflow Water, and Mediterranean Sea Water [*Talley*, 2011]. Oceanographers divide the flow of NADW into three layers: Upper (UNADW), Middle (MNADW), and Lower (LNADW). There is no commonly accepted opinion about the origin of North Atlantic Deep Water components.

The goal of this paper was to analyze the deep flow in the Bear Island Trough based on the data in July–August 2017 and a numerical model. We also compared the measured tides with the existing tidal models based on satellite altimetry.

Data and Methods

On July 23 – August 3, 2017, we occupied two CTD sections across and along the Bear Island Trough in the western Barents Sea. Each section included six stations. We deployed a mooring with an Acoustic Doppler Current Profiler (ADCP) close to the bottom at the point of intersection (station 5528 at 73°15.6′ N, 17°24.6′ E) between these two sections in the deepest part of the Bear Island Trough. The bottom topography along the sections was measured by the Kongsberg EA600 12 kHz single beam echo sounder. The locations of the CTD stations and mooring are shown in Figure 1.

The CTD profiles were measured from the surface to the bottom (3–4 m above the seafloor) using a Sea-Bird SBE 911plus profiler. This CTD system was equipped with two parallel temperature and conductivity sensors; the mean temperature difference between them did not exceed 0.001 °C, while that of salinity was not greater than 0.001 PSU. The raw

CTD data were processed by SBE Data Processing software version 7.23.2 with standard parameters described in [*Sea-Bird Electronics Inc.*, 2014].

We also used the satellite altimetry data and the TPXO9 model [*Egbert and Erofeeva*, 2002] to plot tidal ellipses and analyze tides from the mooring measurements and altimetry.

Results and Discussion

Surface currents in the region of the Bear Island Trough are well studied [*Beszczynska-Möller et al.*, 2012]. Geostrophic currents based on satellite altimetry averaged over 1993–2020 are shown in Figure 2. Atlantic water transported by the North Atlantic Current overflows the Iceland-Scotland Ridge and continues as the Norwegian Atlantic Current. This current maintains a two-branch structure in the Nordic Seas towards the Fram Strait. Both branches follow topography, the eastern branch (the Norwegian Atlantic Slope Current) is a current along the continental slope west of Norway. Part of this flow separates and turns to the north. The western branch of the Norwegian Atlantic Current or Norwegian Atlantic Front Current flows as a topographically guided stream to the Fram Strait. Near Spitsbergen, both branches merge into the West Spitsbergen Current. However, only a part of the West Spitsbergen Current continues into the Arctic Ocean, while a significant amount recirculates in the Fram Strait and returns south to the Nordic Seas [*Schauer et al.*, 2004]. North of Cape Nordkap, the eastern branch (Norwegian Atlantic Slope Current) enters the Barents Sea. Part of the West Spitsbergen Current near Bear Island separates from the main current and turns east. Geostrophic currents based on long term satellite data are shown in Figure 2 and confirm this scheme.

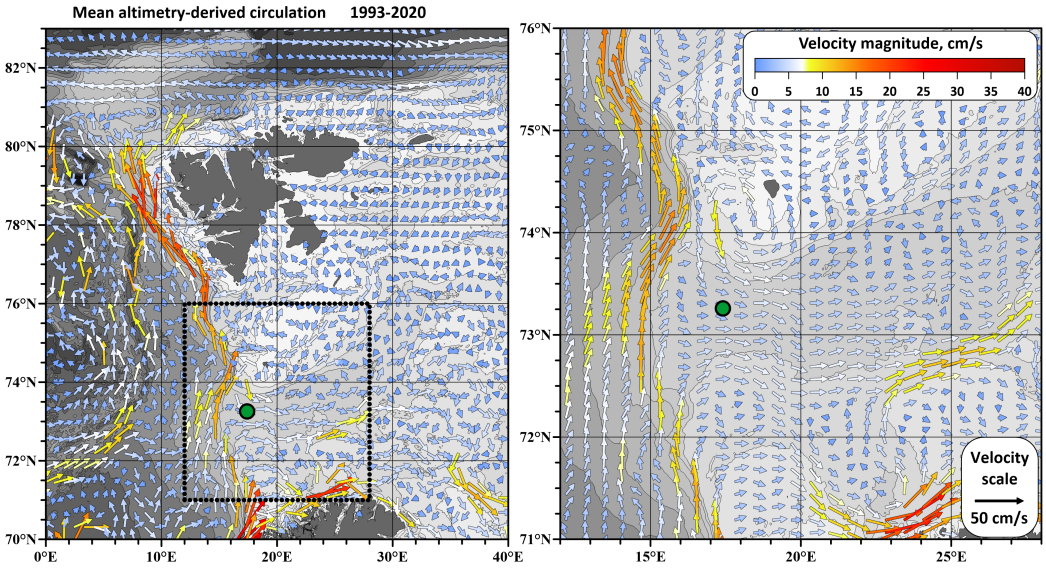

Figure 2. Surface geostrophic currents in the Norwegian Sea based on satellite altimetry averaged over 1993–2020. Part of this map confined by black square is shown in the right panel. The green dot shows location of our mooring in the Bear Island Trough (station 5528).

A similar scheme of currents but based on the altimetry only on the data on July 26, 2017 (the day of our mooring operation) is shown in Figure 3. A distinguishing difference is a stronger southern branch separated from the West Spitsbergen Current west of Bear Island, which turns to the east at 74°N following bottom topography. In addition, the current north of Cape Nordkap is poorly pronounced.

To study the bottom circulation in the region, we applied the Institute of Numerical Mathematics Ocean Model (INMOM) to simulate the circulation in the bottom layer of the Norwegian Sea [*Diansky et al.*, 2002, 2021; *Morozov et al.*, 2019; *Zalesny et al.*, 2012]. This model is based on the system of the so-called primitive ocean hydrodynamic equations in spherical horizontal coordinates. We apply the hydrostatic and Boussinesq approximations and the vertical σ-coordinate system. The results of model simulations are shown in

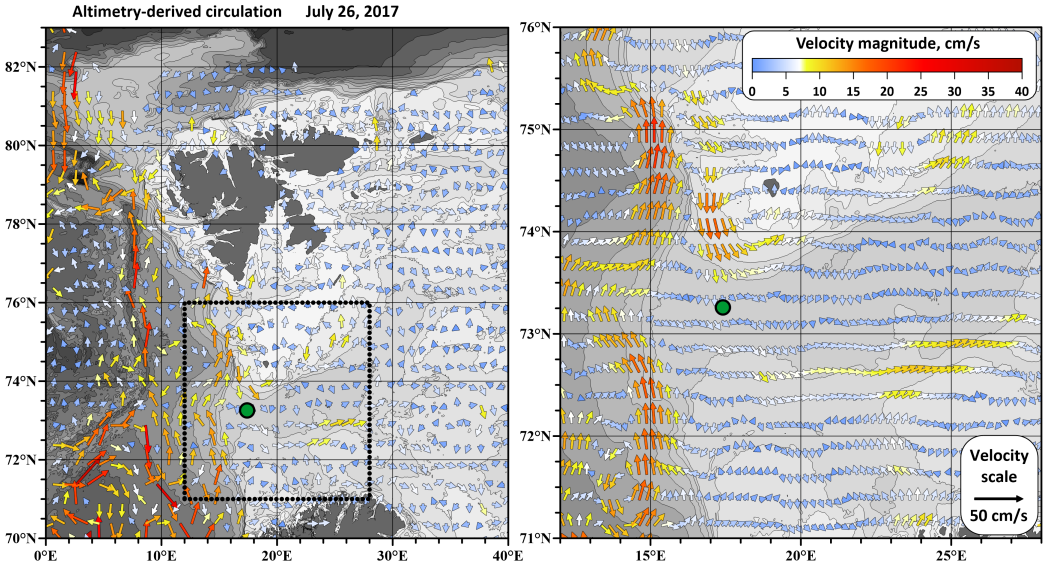

Figure 3. Same as in Figure 2, but on the day of July 26, 2017.

Figure 4, which presents the vectors of currents in the bottom layer in July [*Morozov et al.*, 2019]. Bottom currents are quite weak and generally there are no high-velocity jets in the entire sea except for the bottom stream of the bottom water from the Barents Sea flowing through the Bear Island Trough to the southwest. This bottom stream turns to the north around Spitsbergen. These conclusions are consistent with the conclusions based on the direct measurements in the Bear Island Trough in 2017 [*Frey et al.*, 2017]. The model results for July 2017 are shown in Figure 4.

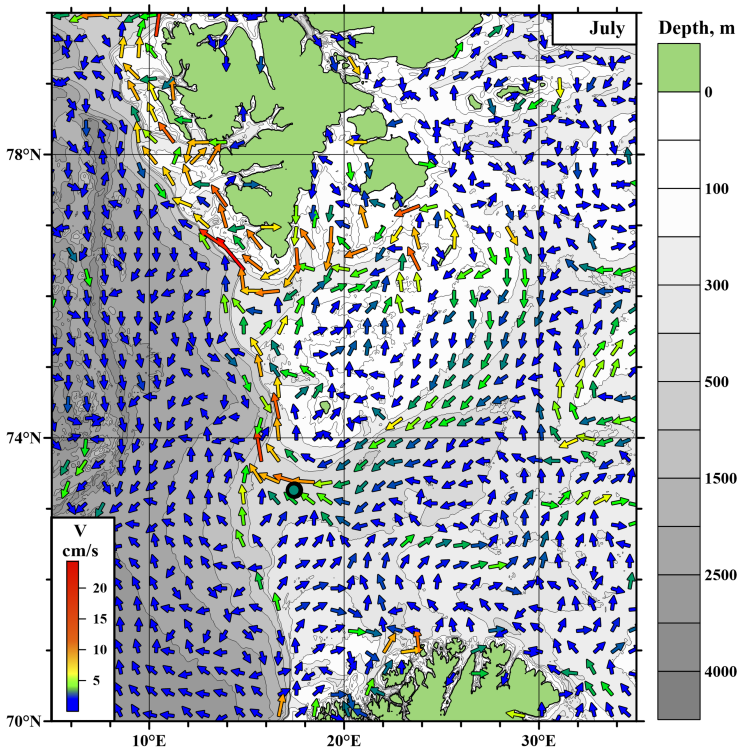

Figure 4. Bottom model currents in the Norwegian Sea based on simulations using the INMOM model for July 2017. The green dot shows the location of our mooring in the Bear Island Trough (station 5528).

This descending flow of cold water in the Bear Island is also illustrated by the water structure over the temperature and salinity sections along the trough. Sections of potential temperature, salinity, and density are shown in Figures 5a, 5b, 5c.

One can see from the figure that a tongue of cold and low saline water descends down the trough. Based on the numerical simulations the velocity of the flow is low. It is of the order of 2–4 cm/s, which gives a time of half a year for a water particle to flow along the trough. In the lower part of the flow the current accelerates, but arrives to the mooring with a lower speed.

The flow in the Bear Island Trough enters the Norwegian Sea at the depths of ~450 m. Thus, the inflowing water appears in the upper part of the water column. The water in the columns up to 850 m deep overflows the Faroe Threshold and becomes part of Iceland-Scotland Overflow Water. Figure 6 shows comparison between the water density in the deep open part of the Norwegian Sea and that in the Bear Island Trough. The water density in the Bear Island Trough is lower than in the open sea because of the excess of freshwater from land, while the water in the open sea is in direct contact with the Arctic Ocean.

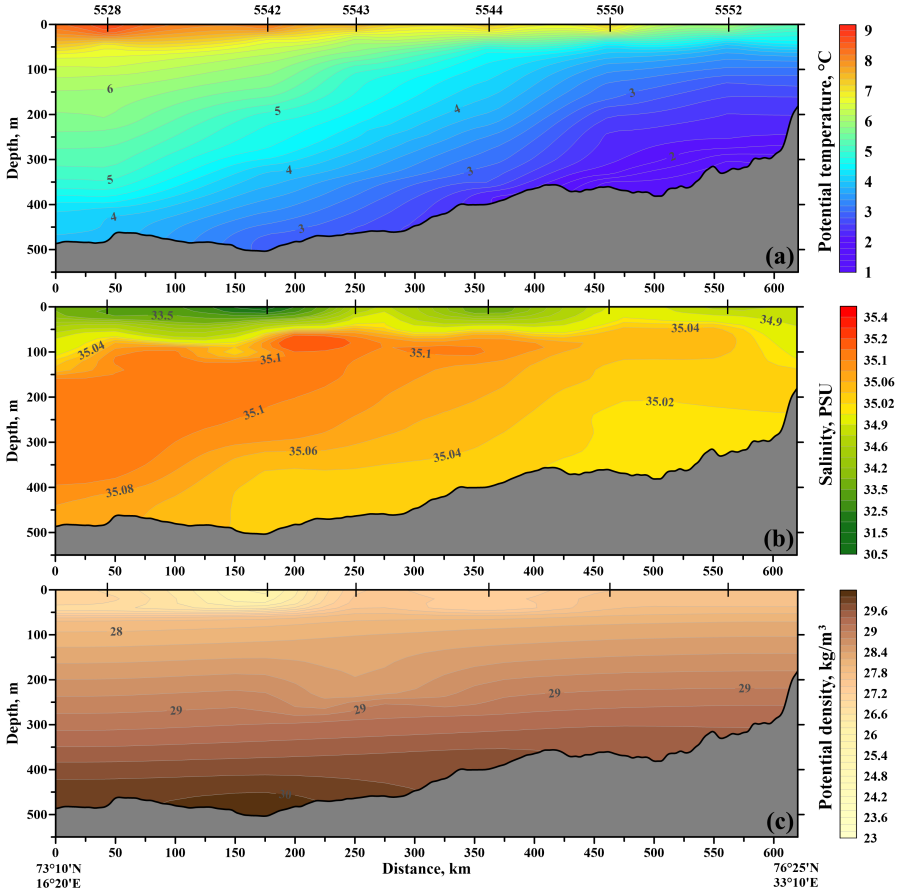

Figure 5. Sections of potential temperature (a), salinity, (b), and sigma-T density (c) along the Bear Island Trough.

No water descent is seen in the density section because the process is density compensated by the process of double diffusion developing over a time period of approximately half a year. Let us estimate whether conditions allow the existence of double diffusion. Double diffusion occurs when cold and low saline water is located above warmer and more saline water. In our case cold, low saline Arctic water descends into the layers of warmer Atlantic water with greater salinity. Thus, the density flux occurs from top to bottom, and the effective density diffusion is positive, which means that the colder water warms [*Kantha and Clayson*, 2000].

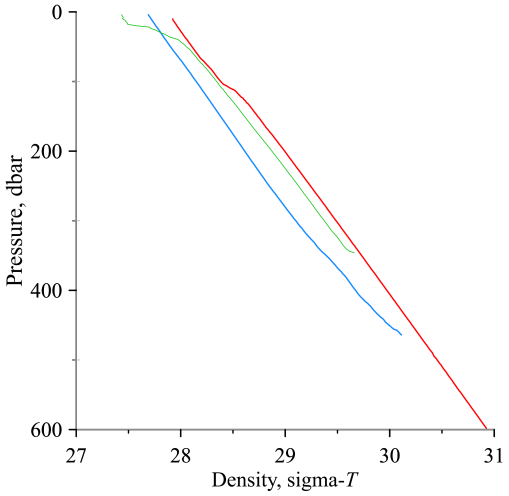

Figure 6. Vertical variation of density at the station in the deep part of the sea at a depth of 3475 m in March 1982 (74.5°N, 4.6°E) (red line) and at stations 5532 (green) and 5550 (blue).

A horizontal flow of colder and less saline water descends in the trough and colder water appears in warmer water of higher salinity. Mechanical mixing occurs, which is accompanied by a faster heat exchange than that with salt and other ions. Warm water of higher salinity in this case ascends. This is a slow process but we estimated the time of the particle motion along the trough as six months, which is enough for this mechanism to be in force.

It was proposed in [*Turner*, 1973] to use the gradient ratio $R_\rho = \alpha T_z/\beta S_z$ to estimate the relative intensity of double diffusion. Here, $\alpha = -\rho^{-1}\partial\rho/\partial T$ is the coefficient of thermal expansion, and $\beta = \rho^{-1}\partial\rho/\partial T$ is the coefficient of salinity compression, ρ is density, and T_z, S_z are vertical gradients of temperature and salinity. The change in density with a change in salinity is approximately 10 times greater than with a change in temperature if they change by one unit. In the ocean, where cold and low saline waters border with warm and salty waters, coefficient R_ρ is close to unity since temperature and salinity have opposite effects on density. Both forms of double diffusion are most intense when coefficient R_ρ is close to unity [*Shi and Wei*, 2007].

Physical parameters are determined from the data of measurements, which makes it possible to study double diffusion structures. Turner angles (Tu) are used to study and classify double diffusion [*Ruddick*, 1983], which are determined by the density coefficient (R_ρ). In our study area in the Bear Island Trough at depths of 300–350 m we have:

$$R_\rho = \frac{\alpha}{\beta}\frac{T_z}{S_z} = 1.9,$$

where, α is the coefficient of thermal expansion, $\alpha = 150 \times 10^{-6}\,/^\circ\mathrm{C}$ for temperatures close to 0 °C; β is salinity compression coefficient is $\beta = -7 \times 10^{-4}$ or 0.7 kg/g. The vertical temperature gradient in the study area at depths of 300–350 m is $T_z = 0.008^\circ\mathrm{C/m}$, the salinity gradient is $S_z = 0.001/\mathrm{m}$. Coefficient $R_\rho = 1.9$ is not very much greater than unity, which gives reason to believe that double diffusion is possible. Double diffusion occurs at positive values of the density ratio R_ρ, that is, in other words, when the vertical gradients of temperature and salinity have the same sign. Density ratio R_ρ is related to the Turner's angle as $R_\rho = \tan Tu$ [*Turner*, 1973]. The most favorable conditions for double diffusion are formed when $R_\rho = 1$ ($Tu = 45^\circ$). In our case $Tu = 60^\circ$ ($\tan 62^\circ = 1.88$).

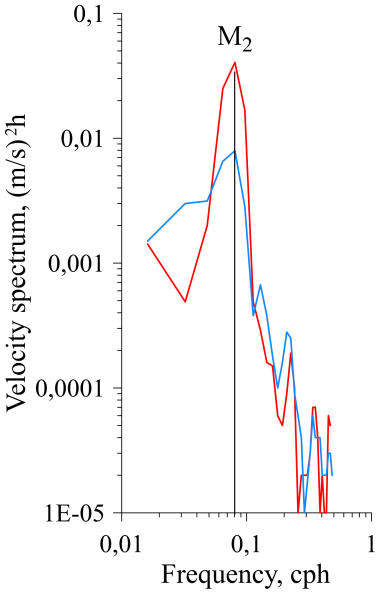

Figure 7. Spectra of velocity fluctuations of the zonal (red) and meridional components (blue) from the mooring.

The mean values of velocity components based on the mooring measurements are $U = -0.04\mathrm{m/s}$, $V = 0.06\mathrm{m/s}$. The study region is characterized by strong tides, which influence the current in the trough and generate strong tidal internal waves, which in turn facilitate mixing [*Morozov*, 2006; *Morozov and Pisarev*, 2002; *Morozov et al.*, 2017]. The spectrum of velocity fluctuations of the zonal and meridional components reveals peaks at the semidiurnal tidal frequency but we cannot separate the M_2 and S_2 constituents because the time series is very short. The spectra of velocity components are shown in Figure 7.

Let us estimate how strong is the tide using the data of measurements and the TPXO9 tidal model [*Egbert and Erofeeva*, 2002] of the Oregon University. We filtered the velocities of the zonal and meridional components so that all other tidal frequencies except the M_2 and S_2 constituents were filtered out. The time period of the ellipses is from July 25, 18:30 to July 27, 06:50. The tidal ellipses are shown in Figure 8 together with the model ellipses for both the M_2 and S_2 constituents. The measured and model ellipses are quite close, which indicates that the TPXO model is adequate.

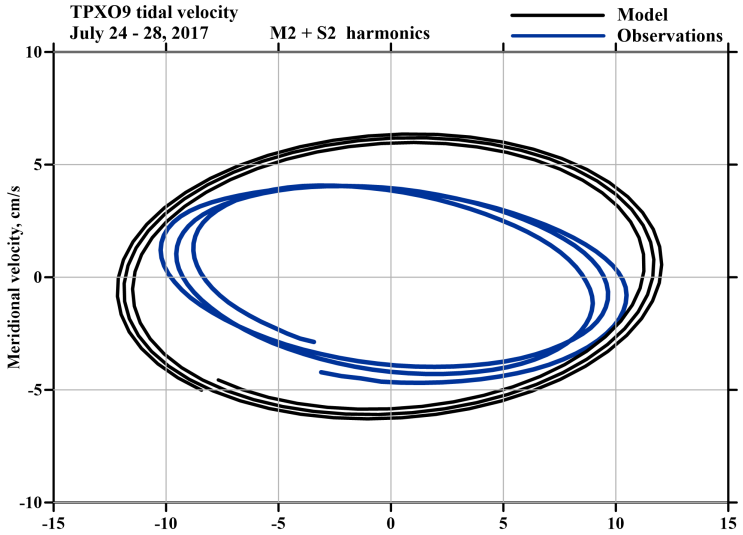

Figure 8. Model (black) and experimental (blue) tidal ellipses. The model ellipses cover a period from July 24 to July 28.

After we subtracted the velocities of the tidal ellipse from the initial data, the mean currents changed from $U = -0.04\,\mathrm{m/s}$, $V = 0.06\,\mathrm{m/s}$, $U = -0.03\,\mathrm{m/s}$, $V = 0.026\,\mathrm{m/s}$. We consider that these values are more reliable than the initial ones that include averaging with tidal velocities. However, the time series is very short but it shows that an opposite mean flow can be present in the trough. Figure 9 illustrates this.

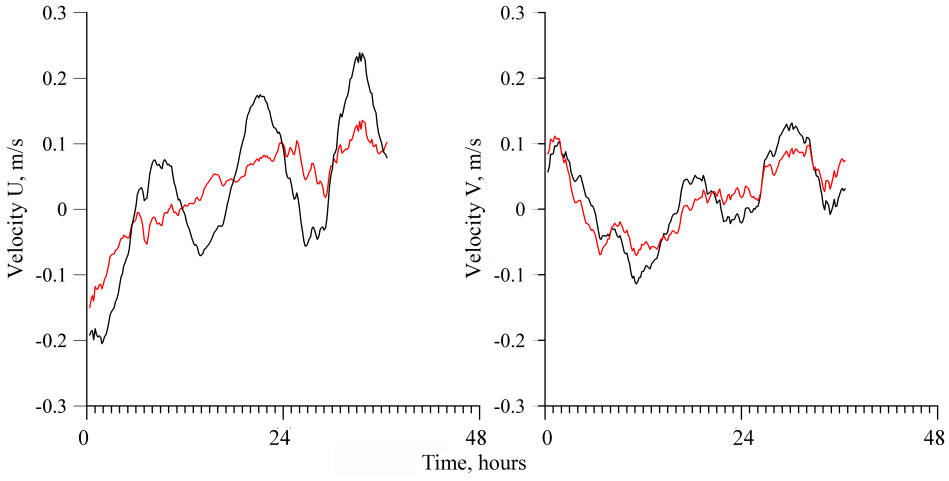

Figure 9. Time series of velocity components (U, left; V, right) before subtracting tidal currents (black) and after subtracting (red).

Figure 10 shows a comparison of the tidal ellipses for four tidal constituents, which indicates that all other constituents are significantly weaker than the M_2 constituent.

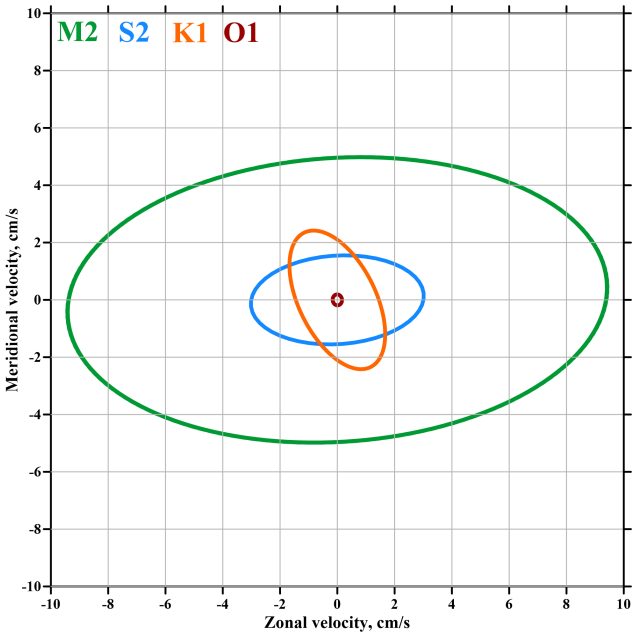

Figure 10. Tidal ellipses for the M_2, S_2, K_1, and O_1 tidal constituents.

Summary and Conclusions

The research deals with oceanographic measurements in the Bear Island Trough, which reveals a flow of Arctic water to the Norwegian Sea. This water becomes part of the Iceland-Scotland Overflow Water. Satellite altimetry was used to map surface geostrophic currents averaged over a long-term period and on the day of measurements. Numerical modeling reveals a bottom current in the trough, which is supported by ADCP measurements on a mooring. Water structure (temperature and salinity sections along the trough) also supports the existence of the bottom flow. Mixing occurs in the trough caused by different processes. Tidal ellipses were calculated from the data of mooring and using the TPXO9 tidal model based on satellite altimetry. The M_2 tide dominates in the region.

Acknowledgments. This work was supported by the State Assignment of the Shirshov Institute of Oceanology (FMWE-2023-0002 analysis of field measurements) and the Russian Science Foundation grant 22-77-10004 (modeling).

References

Aken, H. M. V., and C. J. D. Boer (1995), On the synoptic hydrography of intermediate and deep water masses in the Iceland Basin, *Deep Sea Research Part I: Oceanographic Research Papers*, *42*(2), 165–189, https://doi.org/10.1016/0967-0637(94)00042-Q.

Beszczynska-Möller, A., E. Fahrbach, U. Schauer, and E. Hansen (2012), Variability in Atlantic water temperature and transport at the entrance to the Arctic Ocean, 1997-2010, *ICES Journal of Marine Science*, *69*(5), 852–863, https://doi.org/10.1093/icesjms/fss056.

Diansky, N. A., A. V. Bagno, and V. B. Zalesny (2002), Sigma model of global ocean circulation and its sensitivity to variations in wind stress, *Izvestiya, Atmospheric and Oceanic Physics*, *38*(4), 537–556.

Diansky, N. A., E. G. Morozov, V. V. Fomin, and D. I. Frey (2021), Spread of Pollution from a Bottom Source in the Norwegian Sea, *Izvestiya, Atmospheric and Oceanic Physics*, *57*(2), 197–207, https://doi.org/10.1134/S0001433821020043.

Dickson, R. R., and J. Brown (1994), The production of North Atlantic Deep Water: Sources, rates, and pathways, *Journal of Geophysical Research: Oceans*, *99*(C6), 12,319–12,341, https://doi.org/10.1029/94JC00530.

Egbert, G. D., and S. Y. Erofeeva (2002), Efficient Inverse Modeling of Barotropic Ocean Tides, *Journal of Atmospheric and Oceanic Technology*, *19*(2), 183–204, https://doi.org/10.1175/1520-0426(2002)019<0183:EIMOBO>2.0.CO;2.

Frey, D. I., A. N. Novigatsky, M. D. Kravchishina, and E. G. Morozov (2017), Water structure and currents in the Bear Island Trough in July-August 2017, *Russian Journal of Earth Sciences*, *17*(3), https://doi.org/10.2205/2017ES000602.

Gammelsrød, T., Ø.. Leikvin, V. Lien, et al. (2009), Mass and heat transports in the NE Barents Sea: Observations and models, *Journal of Marine Systems*, *75*(1–2), 56–69, https://doi.org/10.1016/j.jmarsys.2008.07.010.

Giraudeau, J., V. Hulot, V. Hanquiez, et al. (2016), A survey of the summer coccolithophore community in the western Barents Sea, *Journal of Marine Systems*, *158*, 93–105, https://doi.org/10.1016/j.jmarsys.2016.02.012.

Jochumsen, K., D. Quadfasel, H. Valdimarsson, and S. Jónsson (2012), Variability of the Denmark Strait overflow: Moored time series from 1996–2011, *Journal of Geophysical Research: Oceans*, *117*(C12), https://doi.org/10.1029/2012JC008244.

Kantha, L. H., and C. A. Clayson (2000), *Small Scale Processes in Geophysical Fluid Flows*, *Volume 67 (International Geophysics)*, 750 pp., Academic Press.

Koltermann, K. P., A. V. Sokov, V. P. Tereschenkov, et al. (1999), Decadal changes in the thermohaline circulation of the North Atlantic, *Deep Sea Research Part II: Topical Studies in Oceanography*, *46*(1–2), 109–138, https://doi.org/10.1016/S0967-0645(98)00115-5.

Lankhorst, M., and W. Zenk (2006), Lagrangian Observations of the Middepth and Deep Velocity Fields of the Northeastern Atlantic Ocean, *Journal of Physical Oceanography*, *36*(1), 43–63, https://doi.org/10.1175/JPO2869.1.

Lind, S., and R. B. Ingvaldsen (2012), Variability and impacts of Atlantic Water entering the Barents Sea from the north, *Deep Sea Research Part I: Oceanographic Research Papers*, *62*, 70–88, https://doi.org/10.1016/j.dsr.2011.12.007.

Lukashin, V. N., and A. D. Shcherbinin (2007), The nepheloid layer and horizontal sedimentary matter fluxes in the Norwegian Sea, *Oceanology*, *47*(6), 833–847, https://doi.org/10.1134/S0001437007060082.

Mauritzen, C., J. Price, T. Sanford, and D. Torres (2005), Circulation and mixing in the Faroese Channels, *Deep Sea Research Part I: Oceanographic Research Papers*, *52*(6), 883–913, https://doi.org/10.1016/j.dsr.2004.11.018.

Morozov, E. (2006), Internal Tides. Global Field of Internal Tides and Mixing Caused by Internal Tides, in *Waves in Geophysical Fluids*, pp. 271–332, Springer Vienna, https://doi.org/10.1007/978-3-211-69356-8_6.

Morozov, E. G., and S. V. Pisarev (2002), Internal tides at the Arctic latitudes (numerical experiments), *Oceanology*, *42*(2), 153–161.

Morozov, E. G., I. E. Kozlov, S. A. Shchuka, and D. I. Frey (2017), Internal tide in the Kara Gates Strait, *Oceanology*, *57*(1), 8–18, https://doi.org/10.1134/S0001437017010106.

Morozov, E. G., D. I. Frey, N. A. Diansky, and V. V. Fomin (2019), Bottom circulation in the Norwegian Sea, *Russian Journal of Earth Sciences*, *19*(2), 1–6, https://doi.org/10.2205/2019ES000655.

Olsen, S. M., B. Hansen, D. Quadfasel, and S. Østerhus (2008), Observed and modelled stability of overflow across the Greenland-Scotland ridge, *Nature*, *455*(7212), 519–522, https://doi.org/10.1038/nature07302.

Årthun, M., R. B. Ingvaldsen, L. H. Smedsrud, and C. Schrum (2011), Dense water formation and circulation in the Barents Sea, *Deep Sea Research Part I: Oceanographic Research Papers*, *58*(8), 801–817, https://doi.org/10.1016/j.dsr.2011.06.001.

Ruddick, B. (1983), A practical indicator of the stability of the water column to double-diffusive activity, *Deep Sea Research Part A. Oceanographic Research Papers*, *30*(10), 1105–1107, https://doi.org/10.1016/0198-0149(83)90063-8.

Schauer, U., E. Fahrbach, S. Osterhus, and G. Rohardt (2004), Arctic warming through the Fram Strait: Oceanic heat transport from 3 years of measurements, *Journal of Geophysical Research: Oceans*, *109*(C6), https://doi.org/10.1029/2003JC001823.

Sea-Bird Electronics Inc. (2014), *Seasoft V2: SBE Data Processing*.

Shi, J., and H. Wei (2007), Evidence of double diffusion in the East China Sea, *Journal of Marine Systems*, *67*(3–4), 272–281, https://doi.org/10.1016/j.jmarsys.2006.04.017.

Smedsrud, L. H., I. Esau, R. B. Ingvaldsen, et al. (2013), The role of the Barents Sea in the Arctic climate system, *Reviews of Geophysics*, *51*(3), 415–449, https://doi.org/10.1002/rog.20017.

Talley, L. D. (2011), *Descriptive Physical Oceanography*, Elsevier, https://doi.org/10.1016/C2009-0-24322-4.

Turner, J. S. (1973), *Buoyancy Effects in Fluids*, Cambridge University Press, https://doi.org/10.1017/CBO9780511608827.

Zalesny, V. B., N. A. Diansky, V. V. Fomin, S. N. Moshonkin, and S. G. Demyshev (2012), Numerical model of the circulation of the Black Sea and the Sea of Azov, *Russian Journal of Numerical Analysis and Mathematical Modelling*, *27*(1), https://doi.org/10.1515/rnam-2012-0006.